Eur. Phys. J. C 21, 81–91 (2001)
Digital Object Identifier (DOI) 10.1007/s100520100733

THE EUROPEAN PHYSICAL JOURNAL C

Single top production in e^+e^-, e^-e^-, γe and $\gamma\gamma$ collisions

E. Boos[1,2], M. Dubinin[1,2], A. Pukhov[1], M. Sachwitz[2], H.J. Schreiber[2]

[1] Institute of Nuclear Physics, Moscow State University, 119899 Moscow, Russia
[2] DESY Zeuthen, 15738 Zeuthen, Germany

Received: 27 April 2001 / Revised version: 31 May 2001 /
Published online: 19 July 2001 – © Springer-Verlag / Società Italiana di Fisica 2001

Abstract. Single top quark cross section evaluations for the complete sets of tree-level diagrams in the e^+e^-, e^-e^-, γe and $\gamma\gamma$ modes of the next linear collider with unpolarized and polarized beams are performed within the standard model and beyond. From a comparison of all possibilities we conclude that the process $\gamma_+ e^-_{\rm L} \to e^- t\bar{b}$ is extremely favored due to large cross sections, there being no $t\bar{t}$ background, the high degrees of beam polarization, and the exceptional sensitivities to V_{tb} and anomalous Wtb couplings. Similar reasons favor the process $e^-e^- \to e^-\nu_e t\bar{b}$ for probing top quark properties despite a considerably lower cross section. Less favorable are processes like $e^+e^-, \gamma\gamma \to e^-\nu_e t\bar{b}$. Three processes were chosen to probe their sensitivities to anomalous Wtb couplings, with best bounds found for $\gamma_+ e^-_{\rm L} \to e^- t\bar{b}$ and $e^+_{\rm R} e^-_{\rm R} \to e^-\nu_e t\bar{b}$.

1 Introduction

The most massive fermion of the standard model (SM), the top quark, may provide unique possibilities to study the consistency of the SM and the effects of new physics at energies of next linear colliders (LC). Precise calculations of the top production by colliding $e^\pm$ and γ beams are very important for the investigation of its couplings to the gauge bosons and the Higgs bosons of the SM, of two Higgs doublet models and their possible extensions.

In previous studies [1] $e^+e^- \to t\bar{t}$ pair production has been investigated in some details at c.m.s. energies near the threshold ($s^{1/2} \sim 350\,\mathrm{GeV}$), where the best measurements of the top mass and width are expected, and also far above the threshold, "in the continuum", where the top quark currents and electric or magnetic moments can be probed with high precision. Single top production within the SM has been comparatively less studied. In the $2 \to 3$ process the $e^+e^- \to W^+tb$ single top cross section has been calculated below the $t\bar{t}$ threshold [2] while at higher energies [3] most attention was focused on the measurements of the Cabibbo–Kobayashi–Maskawa (CKM) matrix element V_{tb}. In these three particle final state approximations an important class of t-channel diagrams with forward scattered electron has not been taken into account[1]. The calculation of the complete set of diagrams for the four fermion final state process $e^+e^- \to e^-\bar{\nu}_e t\bar{b}$ has been performed for LEP2 energies in [5] and for LC energies in [6,7]. It was concluded that the event rate expected at LEP2 is so small that practically no events would be observed. The analysis of [6] concerns the precision of V_{tb} measurements at LC. There are also single top investigations for γe^- at LC [8] and $p\bar{p}$, pp collisions at Tevatron and LHC [9] energies.

In this paper we evaluate cross sections for e^+e^-, e^-e^-, $\gamma\gamma$ and γe^- collisions to the four fermion final state $e^-\bar{\nu}_e t\bar{b}$, respectively, three fermion final state $\nu_e t\bar{b}$, taking into account the complete sets of tree-level Feynman diagrams. Further, we consider besides unpolarized also polarized initial state particle scattering, so a full comparison of all initial state configurations of a linear collider can be performed. Our analysis for single top production in polarized γe^- collisions goes beyond the study of [8] for the unpolarized case and demonstrates the advantages of beam polarization at LC. All calculations were performed by means of the CompHEP package [10], after implementation of polarized electron, positron and photon states. We consider the energy range from about 350 GeV (where a non-negligible single top event rate at a high-luminosity collider is expected) up to 1 TeV, planned for a first generation LC.

It has been emphasized in e.g. [6] that single top production is sensitive to the V_{tb} matrix element since its rate is proportional to $|V_{tb}|^2$. Futhermore, if anomalous effective operators for the Wtb vertex are introduced, the single top rate is sensitive to them, unlike the $t\bar{t}$ rate. This can be easily understood in the *production* × *decay* approximation for the $t\bar{t}$ amplitude and within the infinitely small top width approximation for the s-channel Breit–Wigner propagator

$$\frac{\int |M(t \to Wb)|^2 \mathrm{d}\Phi}{(q^2 - m^2_{\rm top})^2 + m^2_{\rm top}\Gamma^2_{\rm tot}}$$

[1] Early calculations of the t-channel subset diagrams at TRISTAN energies can be found in [4], where the denomination "single top" has been introduced

Table 1. Top quark production by e^+, e^- and γ beams with various polarizations. The single top quark production cross sections (with $m_{\rm top} = 175\,{\rm GeV}$) are given for the channels $e^-e^+, \gamma\gamma \to e^-\bar{\nu}_e t\bar{b}$, $e^-e^- \to e^-\nu_e t\bar{b}$ and $\gamma e^- \to \nu_e t\bar{b}$ at $s^{1/2}$ =0.5 and 1.0 TeV

Beams	No. of diagrams	Polarization and subset	$t\bar{t}$ production	$\sigma_{\rm single\ top}$, fb $\sqrt{s} = 0.5\,{\rm TeV}$	$\sigma_{\rm single\ top}$, fb $\sqrt{s} = 1\,{\rm TeV}$
e^-e^+	20	unpol	yes	3.1	6.7
	10	unpol,s-ch.	yes	2.3	2.3
	10	unpol,t-ch.	no	0.8	4.4
	20	LR	yes	10.0	16.9
	11	RL	yes	1.7	1.0
	9	RR	no	1.0	8.1
	2	LL	no	-	-
e^-e^-	20	unpol	no	1.7	9.1
	20	LL	no	2.6	19.1
	11	LR	no	2.1	14.0
	11	RL	no	2.1	14.0
	4	RR	no	0.02	0.96
γe^-	4	unpol	no	30.3	67.6
	4	$-$L	no	38.9	121.3
	4	$+$L	no	94.3	174.7
$\gamma\gamma$	21	unpol	yes	9.2	18.8
	21	$(++)$	yes	11.1	19.2
	21	$(--)$	yes	7.9	15.7
	21	$(+-)$ or $(-+)$	yes	8.5	19.2

$$= {\rm Br}(t \to Wb)\Gamma_{\rm tot}\frac{\pi}{m_{\rm top}\Gamma_{\rm tot}}\delta(q^2 - m_{\rm top}^2) \quad , \quad (1)$$

where ${\rm Br}(t \to Wb) = \Gamma(t \to Wb)/\Gamma_{\rm tot} = \int |M(t \to Wb)|^2 {\rm d}\Phi/\Gamma_{\rm tot}$ is always close to 1, and $\Gamma_{\rm tot}$, sensitive to anomalies, cancels out. By way of contrast, simple counting of single top events could reveal signals of anomalous Wtb couplings, and for a running strategy of a linear collider it is worth to perform a comparative study of single top production for all possible collider options, with unpolarized and polarized beams, and to point to the most appropriate collider mode.

Top quark studies in the six fermion final states [11] and their four particle final state approximation $W^+bW^-\bar{b}$ [12] were focused on $t\bar{t}$ pair production. The case of single top quark production was not considered there.

This paper is organized as follows. In Sect. 2 we present the single top quark cross sections for unpolarized and polarized e^+e^-, e^-e^-, γe^- and $\gamma\gamma$ collisions. In Sect. 3 the anomalous CP- and flavor conserving Wtb operators of dimension 6 are introduced and, as examples, possible bounds on anomalous couplings in $e^+_{\rm R}e^-_{\rm R}$, $e^-_{\rm L}e^-_{\rm R}$ and $\gamma_+e^-_{\rm L}$ collisions are discussed. Our conclusions are presented in Sect. 4.

2 Cross sections in the e^+e^-, e^-e^-, γe and $\gamma\gamma$ modes of linear collider

Single top quark production in e^+e^- and $\gamma\gamma$ collisions has to be extracted from the complete sets of tree-level diagrams leading to the four fermion final state $e^-\bar{\nu}_e t\bar{b}$, which is the most general four fermion case. In unpolarized e^+e^- (Figs. 1, and 2) and $\gamma\gamma$ (Fig. 3) collisions this final state appears either from $t\bar{t}$ pair production with the top decay into $e^-\bar{\nu}_e\bar{b}$ (see diagrams 3,4 in Fig. 1 and diagrams 6,7 in Fig. 3) or from single top production in association with the $e^-\bar{\nu}_e\bar{b}$ system. After the elimination of $t\bar{t}$ pair production by means of a subtraction procedure (see Sect. 2.1) all diagrams in Figs. 1–3 contribute to single top production. In e^-e^- (Fig. 4) and γe^- collisions (Fig. 5) only single top quark production is possible.

Appropriate beam polarization gives the possibility to exclude $t\bar{t}$ pair production in the e^+e^- case and allows for only single top quark production. Such a possibility does not exist for $\gamma\gamma$ collisions, whatever polarizations one assumes.

Table 1 summarizes the various possibilities expected for a linear collider. Discussions of single top quark production cross sections for all collision modes offered by a LC are presented in the following.

2.1 Single top production in e^+e^- collisions with unpolarized and polarized beams

In order to calculate at complete tree level the single top cross section in the reaction $e^-e^+ \to e^-\bar{\nu}_e t\bar{b}$[2] with unpolarized beams, all 20 Feynman diagrams of Figs. 1 and 2 have to be taken into account to ensure gauge invariance. The diagrams in these figures form two minimal [14]

[2] The final states $\mu\nu_\mu t\bar{b}$ and $\tau\nu_\tau t\bar{b}$ produce single top events with the same rate as the $CC10$ s-channel diagrams of Fig. 1. The definitions of $CC10$ and $CC20$ are given in [13]

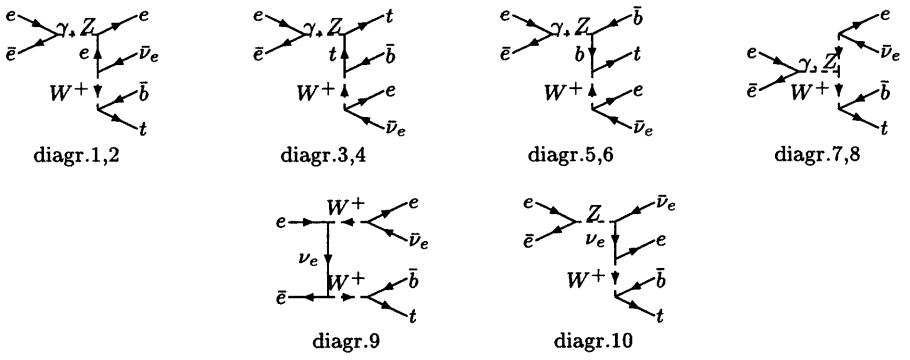

Fig. 1. s-channel $CC10$ diagrams for the process $e^-e^+ \to e^-\bar{\nu}_e t\bar{b}$, unpolarized beams

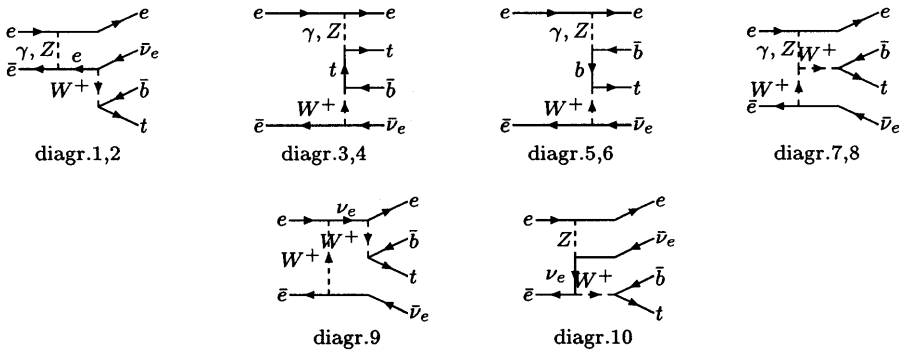

Fig. 2. t-channel $CC10$ diagrams for the process $e^-e^+ \to e^-\bar{\nu}_e t\bar{b}$, unpolarized beams

gauge invariant subsets. The energy dependence of the cross sections for the entire $e^-e^+ \to e^-\bar{\nu}_e t\bar{b}$ reaction and the s- and t-channel subsets is shown in Fig. 6a. Most of the $e^-e^+ \to e^-\bar{\nu}_e t\bar{b}$ cross section comes from the s-channel diagrams which in turn are dominated by $t\bar{t}$ pair production (diagrams 3,4 in Fig. 1). This contribution has to be subtracted from the total event rate in a gauge invariant manner to get the single top rate.

We define the single top cross section as the difference of the complete tree-level (CTL) contribution and the Breit–Wigner (BW) resonance contribution $\int \mathrm{d}M_{e\nu b}$ $(\mathrm{d}\sigma^{\mathrm{CTL}}/\mathrm{d}M_{e\nu b} - \mathrm{d}\sigma^{\mathrm{BW}}/\mathrm{d}M_{e\nu b})$.

However, for simplicity we applied a cut on the $e\nu b$ invariant mass around the top quark pole [6,15] as an equivalent of the BW subtraction procedure,

$$\sigma = \int\limits_{M_{\min}}^{m_{\mathrm{top}}-\Delta} \mathrm{d}M_{e\nu b} \frac{\mathrm{d}\sigma^{\mathrm{CTL}}}{\mathrm{d}M_{e\nu b}} + \int\limits_{m_{\mathrm{top}}+\Delta}^{M_{\max}} \mathrm{d}M_{e\nu b} \frac{\mathrm{d}\sigma^{\mathrm{CTL}}}{\mathrm{d}M_{e\nu b}}, \quad (2)$$

where the value of Δ is adjusted to compensate for the small amount of discarded single top events inside the interval $m_{\mathrm{top}} - \Delta \le m_{\mathrm{top}} \le m_{\mathrm{top}} + \Delta$ by the remaining top Breit–Wigner tails outside. The cross sections obtained using (2) have been compared with those based on a subtraction of $t\bar{t}$ cross sections from a fit of a Breit–Wigner function superimposed with a polynomial to $M_{e\nu_e b}$. Both numbers agree very well if Δ is taken to be 20 GeV. This value of Δ is much larger than an intuitively expected one of the order of the top quark width, which would lead to large contributions of surviving $t\bar{t}$ events. Obviously, the procedure applied is gauge invariant. The resulting single top cross section for unpolarized e^+e^- collisions is shown in Fig. 7 (solid curve). Below the $t\bar{t}$ threshold it is less than 1 fb and increases up to 7 fb at $s^{1/2} = 1$ TeV.

It is interesting to compare the case of single top production at LC with the case of single W production at LEP2. If one replaces the top and b quarks in Figs. 1 and 2 by light quarks, $(t, b \to u, d)$, one gets exactly the $CC20$ diagrams which were used to study single W production at LEP2 [16]. Since the $t\bar{t}$ cross section at a linear collider is much larger than the single top cross section (for $s^{1/2} \ge 350$ GeV), we anticipate a situation similar to the case of single W production when the W signal has to be isolated from the large W^+W^- pair background. Single W isolation at LEP2 can be achieved by simple cuts on the forward going electron which separate the t-channel diagram subset and minimizes interferences, as concluded from rather extensive analyses [16]. However, the LEP2 single W isolation procedure cannot be simply repeated in our case. The single top cross section shown in Fig. 7 for unpolarized e^+e^- collisions is larger than those of the t-channel subset (see Fig. 6a), especially at lower energies, due to considerable single top contributions from the s-channel subset (Fig. 1). Thus, the separation of events from only the t-channel gauge invariant subset by cuts on a forward electron as done at LEP2 would significantly underestimate the single top cross section. This rate is underestimated by e.g. more than 60% at $s^{1/2} = 0.5$ TeV and by about 30% at $s^{1/2} = 1$ TeV, in comparison with the rates obtained from the invariant mass subtraction

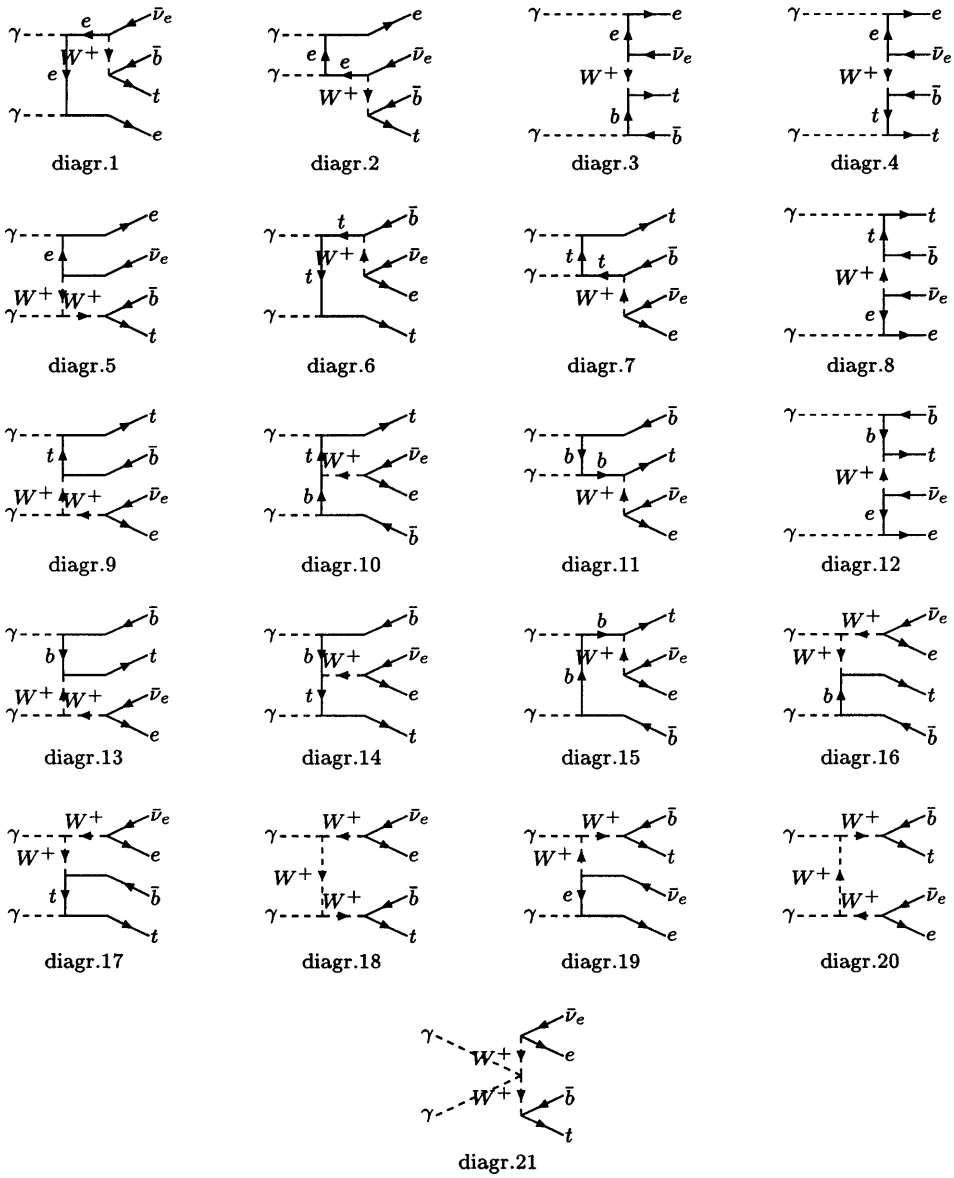

Fig. 3. Diagrams for the process $\gamma\gamma \to e^-\nu_e\bar{t}b$

procedure. The reason can be qualitatively understood as follows. The application of cuts on a forward electron dramatically suppresses the $CC10$ s-channel diagrams in both the W and top cases. Since, however, the ratio of single W to W^+W^- pair cross sections in the s-channel subset is significantly smaller than the corresponding single top to $t\bar{t}$ ratio, the relative contribution of the $CC10$ s-channel top diagrams is enhanced.

The availability of longitudinally polarized beams at a linear collider opens a new window for single top quark studies.

In the case of left-handed e^- with right-handed e^+ collisions, $e^-_{\rm L}e^+_{\rm R}$, all 20 diagrams of Figs. 1 and 2 contribute to the total top quark production with a rate three times higher than for the unpolarized case, see Fig. 6b, for the entire reaction $e^+e^- \to e^-\bar{\nu}_e t\bar{b}$. The single top event rate obtained from the mass cut subtraction procedure is also increased by a factor of three (Fig. 7), and the energy behavior resembles, as expected, the unpolarized cross section increase, reaching 17 fb at 1 TeV.

If right-handed electrons collide with left-handed positrons, $e^-_{\rm R}e^+_{\rm L}$, only 11 diagrams of Figs. 1 and 2 survive. They form two gauge invariant subsets: the t-channel subset of two diagrams (diagrams 1 and 2 in Fig. 2), and the s-channel subset of 9 diagrams (diagrams 1–8 and 10 in Fig. 1). The single top cross section energy behavior, also shown in Fig. 7, reveals, after a broad maximum around 500 GeV, a slow decrease with increasing energy. This happens because the important multiperipheral diagrams 3–8 in Fig. 2, responsible for the increase of the event rate, are removed by orthogonal helicity projectors in the initial left-handed positron state and the W boson (V–A) interaction vertex.

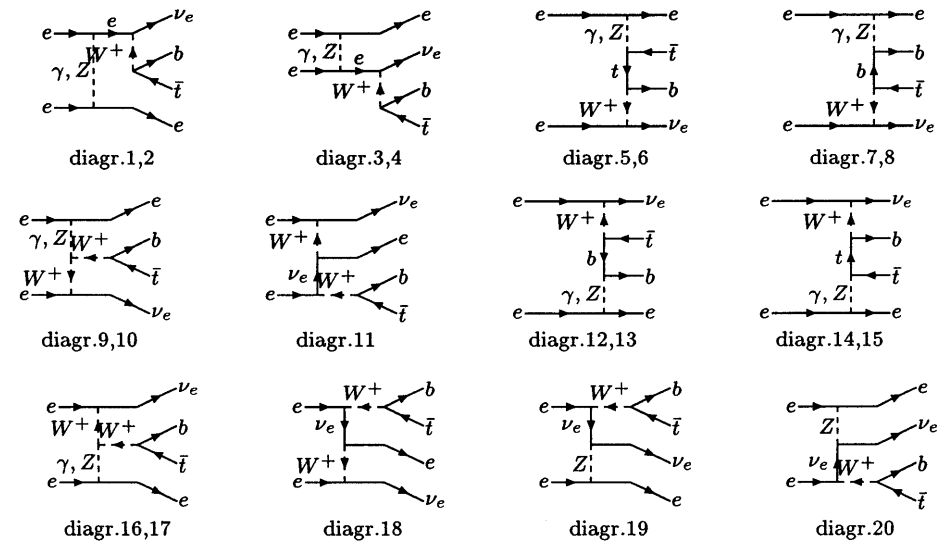

Fig. 4. Diagrams for the process $e^-e^- \to e^-\nu_e\bar{t}b$, unpolarized beams

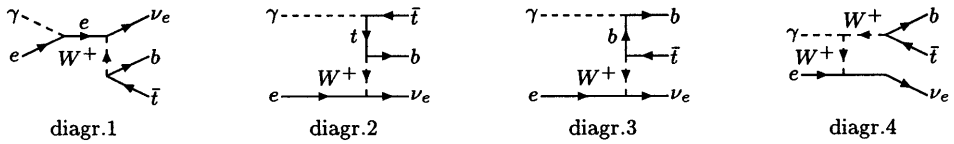

Fig. 5. Diagrams for the process $\gamma e \to \nu_e\bar{t}b$

If both beam particles collide with right-handed polarizations, $e^-_{\rm R}e^+_{\rm R}$, only a gauge invariant subset of 9 diagrams contribute (all diagrams in Fig. 2 except diagram 9). Hence, this helicity configuration avoids a priori the $t\bar{t}$ background and would provide a good laboratory for single top quark physics. Cross sections are large enough for precise measurements, see Fig. 7, being close to 1 fb at $s^{1/2} = 0.5\,\text{TeV}$ respectively 8 fb at $s^{1/2} = 1\,\text{TeV}$.

For completeness it is worth mentioning that $e^-_{\rm L}e^+_{\rm L}$ collisions involve only two diagrams (diagrams 1,2 in Fig. 2) with negligibly small cross sections due to unfavorable helicity configurations. They are formed by means of the left-handed projector of the initial positron and the left-handed $e^-\nu_e$ vector current.

It is important to point out that for both unpolarized and opposite-polarized e^+e^- collisions the dominating $t\bar{t}$ event rates have to be subtracted from the total rate, resulting in additional statistical uncertainties for single top cross section measurements. For example, in the unpolarized e^+e^- case at $s^{1/2} = 500\,\text{GeV}$ and an integrated luminosity of $500\,\text{fb}^{-1}$ the relative single top cross section error $\delta\sigma/\sigma$ increases by 8.2%.

In summary, in e^+e^- collisions single top quark production is largest for the $e^-_{\rm L}e^+_{\rm R}$ case, but its experimental precision is diluted by additional statistical uncertainties from the $t\bar{t}$ subtraction procedure. $e^-_{\rm R}e^+_{\rm R}$ collisions avoid a priori the $t\bar{t}$ background and yield, in particular at large $s^{1/2}$, cross sections of a few fb, which is sufficient for precise measurements at a high-luminosity collider. However, this statement should be somewhat qualified due to partial beam polarizations in real experiments. For collisions of e.g. 80% right-polarized electrons with 60% right-polarized positrons we expect significant $t\bar{t}$ contaminations from $e^-_{\rm R}e^+_{\rm L}$ and $e^-_{\rm L}e^+_{\rm R}$ initial states of 44.1 (14.9) fb at 0.5 (1.0) TeV. These values should be compared with the expected single top cross sections of 8.6 and 12.1 fb, respectively, so that due to imperfect beam polarizations

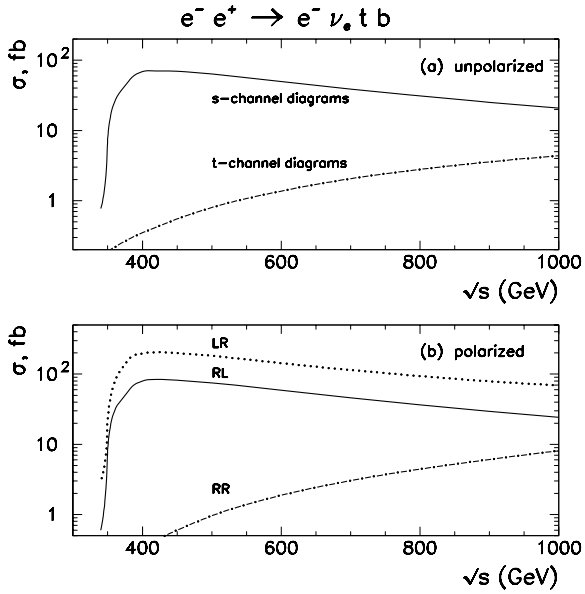

Fig. 6a,b. Energy dependence of the cross sections for the process $e^+e^- \to e^-\bar{\nu}_e t\bar{b}$ for **a** unpolarized e^+e^- s- and t-channel gauge invariant subsets and **b** fully polarized beams

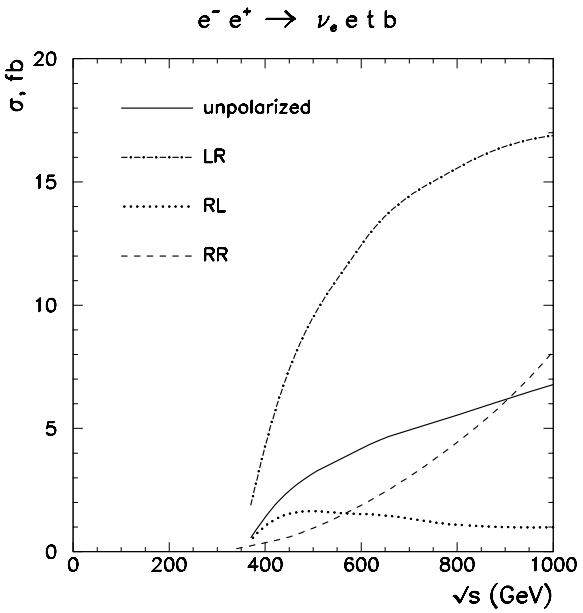

Fig. 7. Energy dependence of the cross section for single top quark production in the process $e^+e^- \to e^-\bar{\nu}_e t\bar{b}$, for unpolarized and fully polarized beams

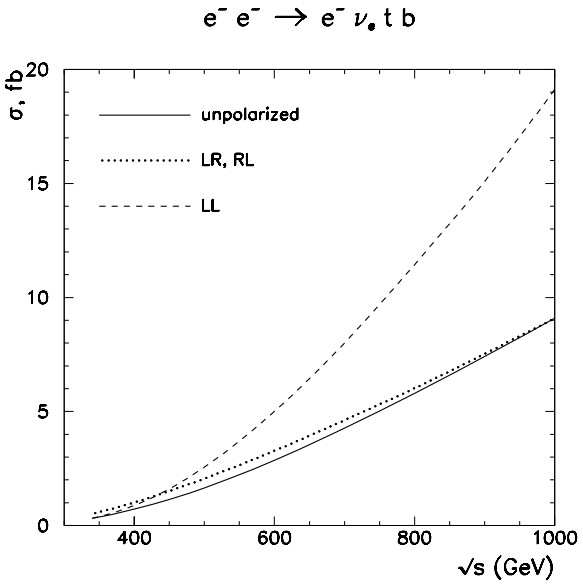

Fig. 8. Energy dependence of the cross section for the processes $e^-e^- \to e^-\nu_e t\bar{b}$, for unpolarized and fully polarized beams

the $e^-_{\rm R}e^+_{\rm R}$ configuration turns out to be very similar to the unpolarized, right–left or left–right configurations at least at $s^{1/2} = 0.5\,\text{TeV}$.

2.2 Single top production in e^-e^- collisions with unpolarized and polarized beams

Due to charge conservation no s-channel γ, Z diagrams are possible in e^-e^- collisions. Consequently, in the reaction $e^-e^- \to e^-\nu_e t\bar{b}$ the top quark is only singly produced. If both electrons are unpolarized, 20 diagrams shown in Fig. 4 contribute. The energy dependence of the cross section is shown in Fig. 8. It grows from almost 2 fb at 0.5 TeV and to 19 fb at 1.0 TeV. Thus, at a high-luminosity e^-e^- collider precise single top cross section measurements can be performed, with the advantage of no need to subtract a large $t\bar{t}$ background.

The cross section for collisions of left-handed and right-handed electrons, $e^-_{\rm L}e^-_{\rm R}$, also shown in Fig. 8, is very close to the unpolarized case. Here only 11 diagrams (1–10 and 19 in Fig. 4) out of the 20 survive.

If both electrons are left-handed polarized, $e^-_{\rm L}e^-_{\rm L}$, all 20 diagrams of Fig. 4 contribute as in the unpolarized case, but the cross section is larger by a factor of two. Since e^- beams can be easily polarized to a high degree (more than 80% at SLAC routinely and this may well be increased to 90% by the time the LC is built), $e^-_{\rm L}e^-_{\rm L}$ scattering is very well suitable for single top cross section measurements with high precision. Right-polarized electron collisions, $e^-_{\rm R}e^-_{\rm R}$, with only yields from diagrams 1–4 in Fig. 4, give however a cross section 50 times smaller than $e^-_{\rm L}e^-_{\rm L}$ collisions (see Table 1).

We would like to mention that e^+e^- and e^-e^- single top event rates are comparable. In the e^+e^- case, significant s- and t-channel contributions were found, contrary to the e^-e^- case where only t-channel diagrams exist. One might expect that e^-e^- collisions are more sensitive to effects of new physics (e.g. to anomalous Wtb couplings), insofar as, in general, t-channel topologies have larger sensitivities to nonstandard vertices than the s-channel ones.

In the SM the Wtb coupling is proportional to the CKM matrix element V_{tb}. Assuming $100\,\text{fb}^{-1}$ integrated luminosity and full reconstruction efficiency, about 200 events expected at $s^{1/2} = 500\,\text{GeV}$ would allow one to measure V_{tb} with an uncertainty of 7% at the 2σ level. This accuracy is of the same order as expected from Tevatron and LHC experiments [17].

2.3 Single top production in γe collisions with unpolarized and polarized beams

The γe mode of a linear collider offers unique properties in favor of single top quark physics in the reaction $\gamma e \to \nu_e t\bar{b}$. No $t\bar{t}$ background exists, the cross section for unpolarized collisions is large [8,18], high degree of beam polarizations is possible and the number of contributing diagrams (Fig. 5) is only four. For these reasons, the potential sensitivity to the Wtb coupling is expected to be high. In this paper we extend previous studies [8,18] to collisions of polarized electrons with either unpolarized or polarized $(+,-)$ photons. Cross sections for unpolarized beams and polarized photons colliding with left-handed electrons are shown in Fig. 9. If electrons are unpolarized, the corresponding polarized cross sections must be divided by two. The most favored case of $\gamma_+e^-_{\rm L}$ collisions has the rate of approximately 100 (180) fb at 0.5 (1.0) TeV. Cross sections with right-handed electrons are suppressed by a factor of the order m_e^2/s and thus negligibly small (unfavorable helicity configuration).

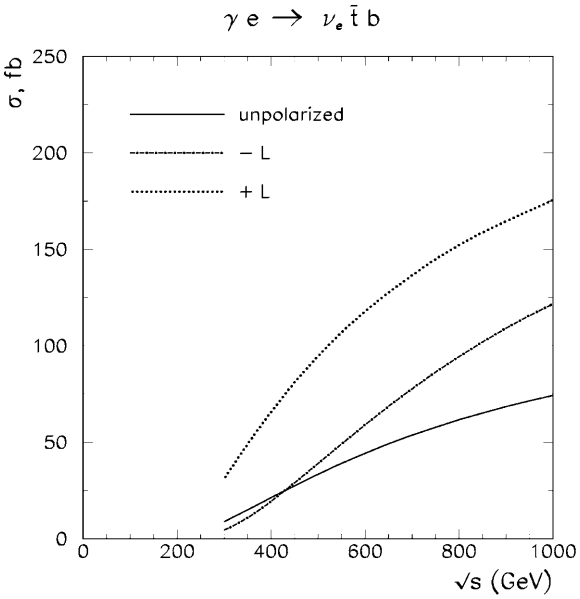

Fig. 9. Energy dependence of the cross section for the process $\gamma e^- \to \nu_e \bar{t} b$, for unpolarized and fully polarized beams

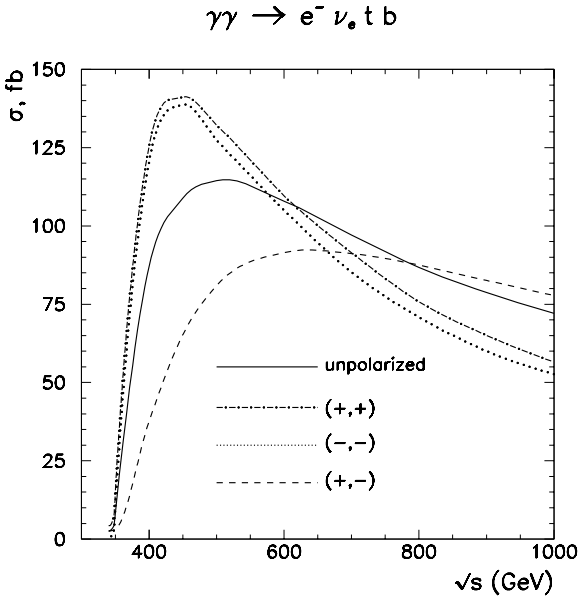

Fig. 10. Energy dependence of the cross section for the process $\gamma\gamma \to e^- \bar{\nu}_e t \bar{b}$, for unpolarized and fully polarized beams

With 10^4 events from $\gamma_+ e^-_{\rm L}$ collisions at $s^{1/2}$=0.5 TeV, expected for 100 fb^{-1} integrated luminosity and no event loss, we measure V_{tb} with an uncertainty of 1% at the 2σ level. This excellent precision can be achieved neither at the Tevatron nor the LHC and from a LC top quark width measurement at the $t\bar{t}$ threshold, with anticipated uncertainties of approximately 5% [17] respectively 10% [19]. In summary, the reaction $\gamma e \to \nu_e \bar{t} b$ with unpolarized or properly polarized beams is extremely suitable for precise measurements of important top quark properties.

2.4 Single top production in $\gamma\gamma$ collisions with unpolarized and polarized beams

Additional possibilities of single top quark production are offered by the $\gamma\gamma$ mode of a linear collider. The reaction $\gamma\gamma \to e^- \bar{\nu}_e t \bar{b}$ however is dominated by $t\bar{t}$ pair production for all initial polarization states possible, and requires always $t\bar{t}$ subtraction to obtain the single top production rate. All contributing diagrams are shown in Fig. 3. Unlike the e^+e^- case, there are no gauge invariant subsets within the complete set of 21 diagrams. The total cross sections of the reaction $\gamma\gamma \to e^- \bar{\nu}_e t \bar{b}$ for unpolarized and polarized beams are shown in Fig. 10, and the $t\bar{t}$ subtracted single top quark production rates in Fig. 11. Obviously, a preferred photon helicity configuration is not evident from Fig. 11. In comparison to e^+e^- and e^-e^- collisions, single top cross sections in $\gamma\gamma$ collisions are enhanced, in particular at energies around 500 GeV. However, this advantage is expected to be degraded by the lower luminosity of a Compton collider.

It is worthwhile to compare single top production in gamma–gamma collisions at LC with single top production in gluon–gluon partonic subprocess at the LHC [15, 20] since they yield the same final state $e^- \nu_e t \bar{b}$. The $t\bar{t}$ pair production part in gg collisions is removed by means of the same gauge invariant subtraction procedure as described in Sect. 2.1. However, another problem in the case of gg collisions is the double counting in the sum of the $gg \to tWb$ and the $gb \to tW$ partonic subprocesses, and a gauge invariant subtraction of the $g \to b\bar{b}$ splitting term is necessary to avoid it. One might expect that a similar double counting problem arises in the case of $\gamma\gamma$ collisions if one includes the "resolved photon" contribution, when the b constituent of the first "resolved photon" collides with

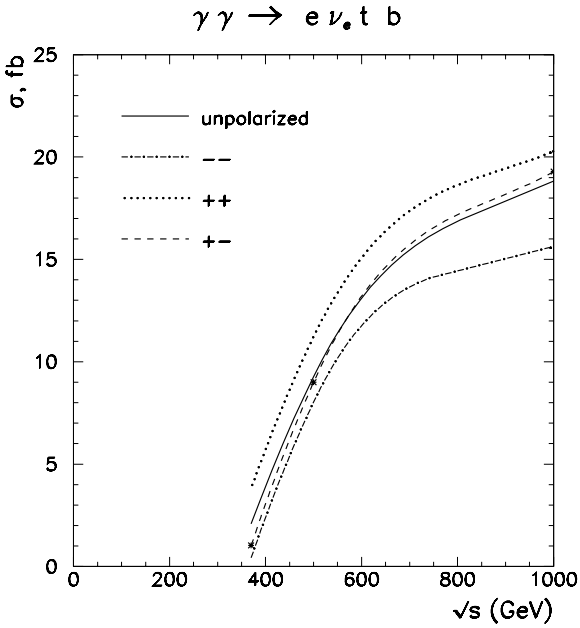

Fig. 11. Energy dependence of the cross section for single top production in the process $\gamma\gamma \to e^- \bar{\nu}_e t \bar{b}$, for unpolarized and fully polarized beams

the second photon. The yield of "resolved photon" (with poorly known gluon and b contents) is however expected to be very small at the characteristic momentum transfer scale $Q^2 \sim m_b^2$. So, the problem of double counting in $\gamma\gamma$ collisions is not expected to be important compared to gg collisions.

3 Single top production with anomalous effective operators of the third generation quarks

Single top quark production at linear colliders is thought to be a promising tool to probe the Wtb vertex. Simple counting of single top events is sensitive to anomalous Wtb couplings, unlike the $t\bar{t}$ pair production where deviations from the SM are difficult to notice. A sophisticated combination of e.g. forward–backward, spin–spin and energy asymmetries is needed to probe couplings in the Wtb vertex ([21], see also [22]).

In the following we demonstrate the sensitivity to anomalous Wtb couplings for the single top quark reactions $e^+_{\rm R}e^-_{\rm R} \to e^-\bar{\nu}_e t\bar{b}$, $e^-_{\rm L}e^-_{\rm R} \to e^-\nu_e t\bar{b}$ and $\gamma_+ e^-_{\rm L} \to \nu_e t\bar{b}$, which, as outlined in Sect. 2, are very promising for this task. Their amplitudes are directly proportional to the Wtb coupling and $t\bar{t}$ background is absent.

In order to probe anomalous Wtb couplings in a model independent way, we use the effective Lagrangian of dimension 6 as proposed in [23]

$$\mathcal{L} = \frac{g}{\sqrt{2}}\frac{1}{2m_W} W_{\mu\nu}\bar{t}\sigma^{\mu\nu}(f_{2\rm R}P_{\rm L} + f_{2\rm L}P_{\rm R})b + \text{h.c.} \quad (3)$$

Here $f_{2\rm L}$ and $f_{2\rm R}$ are the anomalous couplings, $W_{\mu\nu} = D_\mu W_\nu - D_\nu W_\mu, D_\mu = \partial_\mu - {\rm i}eA_\mu$, $P_{\rm L,R} = 1/2(1 \pm \gamma_5)$ and $\sigma_{\mu\nu} = {\rm i}(\gamma_\mu\gamma_\nu - \gamma_\nu\gamma_\mu)/2$.

Calculations of diagrams with photons in the t-channel using the effective Wtb vertex (3) should be carefully performed. It follows from existing experience that the direct introduction of Breit–Wigner propagators with finite width in the amplitude could break the unitary behavior of the single top cross section. Unitary behavior is ensured by the cancellation of the double pole $1/t^2$ behavior of the individual photon exchange squared diagrams to the single pole $1/t$ behavior of the squared amplitude[3]. This cancellation is controlled by the electromagnetic $U(1)$ gauge invariance. The violation of the $U(1)$ invariance is usually made manifest as a several orders of magnitude cross section increase [24,26] for very small electron scattering angles in obvious contradiction with the unitary cross section behavior. The violation of unitary behavior is well known from analyses of single W production in the SM [24] and various prescriptions to circumvent this difficulty were proposed (see for instance [25] and references therein). We are using the process-independent *overall* prescription for Breit–Wigner propagators (for details see [13,24,25]).

[3] It is important to point out that additional 4-point vertices γWtb appear due to covariant derivatives in the $W^\pm_{\mu\nu}$ tensor (see [8] for details)

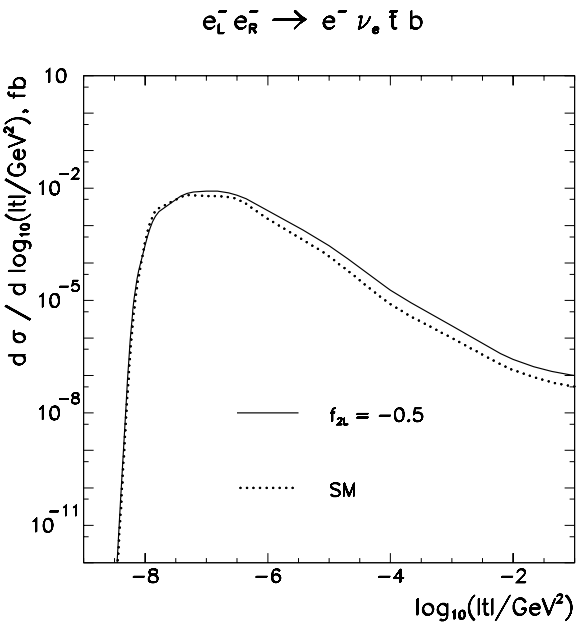

Fig. 12. Distributions in the logarithm of the t-channel photon momentum transfer squared for the process $e^-_{\rm L}e^-_{\rm R} \to e^-\nu_e\bar{t}b$ in the SM and for the anomalous couplings $f_{2\rm L} = -0.5$ and $f_{2\rm R} = 0$

The cancellation of the $1/t^2$ pole can be checked directly by inspection of the differential cross section ${\rm d}\sigma/{\rm dlog}(t) = t{\rm d}\sigma/{\rm d}t$ [25,26]. As an example, this cross section is shown in Fig. 12 for the process $e^-_{\rm R}e^-_{\rm L} \to e^-\nu_e\bar{t}b$. At small $|t|$ near the pole, the distribution for the anomalous couplings $f_{2\rm L} = -0.5$, $f_{2\rm R} = 0$ is only marginally different in comparison with the SM cross section ($f_{2\rm L} = f_{2\rm R} = 0$), so the cancellation of the double pole indeed occurs.

Calculations with different values for $f_{2\rm L}$ and $f_{2\rm R}$ were performed for the three reactions mentioned above, mostly at $s^{1/2} = 500\,{\rm GeV}$ and for two values of integrated luminosity. The 2σ bounds of the anomalous coupling parameter space, within which no distinction from the SM is possible, are shown in Fig. 13. Best bounds for $f_{2\rm L}$ can be obtained from the reaction $\gamma_+e^-_{\rm L} \to \nu_e\bar{t}b$, $-0.02 \le f_{2\rm L} \le 0.06$, being relatively independent of the integrated luminosity. In comparison to unpolarized γe^- collisions [8], the beam polarizations restrict the allowed range of $f_{2\rm L}$ by a factor of 2 to 3, but have no impact on $f_{2\rm R}$. The coupling $f_{2\rm R}$ is almost equally well bounded to $-0.1 \le f_{2\rm R} \le 0.1$ by $e^-_{\rm R}e^+_{\rm R}$ and $\gamma_+e^-_{\rm L}$ collisions at 500 GeV for $100\,{\rm fb}^{-1}$ integrated luminosity. Improvements for $f_{2\rm R}$ can be achieved by e.g. a five times higher luminosity in either the $e^-_{\rm L}e^-_{\rm R}$ or the $e^-_{\rm R}e^+_{\rm R}$ case, with best 2σ bounds of $-0.05 \le f_{2\rm R} \le 0.05$ from the reaction $e^-_{\rm R}e^+_{\rm R} \to e^-\bar{\nu}_e t\bar{b}$. Here, doubling the c.m.s. energy affects $f_{2\rm R}$ in the same way as an increase of the integrated luminosity from $100\,{\rm fb}^{-1}$ to $500\,{\rm fb}^{-1}$.

The introduction of effective operators with the top quark is usually motivated by the expectations that the SM is an effective theory at the electroweak scale for some underlying new physics at higher energies. Anomalous interactions of the third generation fermions (t, b) are introduced by most general local $SU(3) \times SU(2) \times U(1)$

invariant effective Lagrangian terms including also Higgs and gauge bosons. In principle, various effective operators can be constructed. A recent discussion of operators with dimension 4 and 5 can be found in [27]. They are strongly constrained by the experimental data on b quark decays and do not contribute to top quark cross sections at a level sufficient for experimental observation. However, for the CP and flavor conserving effective operators of dimension 6 the limits from experimental data are weaker or even missing. In the notation of [28] seven effective operators ($SU(3) \times SU(2) \times U(1)$ invariant before the electroweak symmetry breaking) provide the anomalous contributions to the Wtb vertex: O_{qW}, $O^3_{\Phi q}$, O_{Db}, $O_{bW\Phi}$, O_{Dt}, $O_{tW\Phi}$, O_{t3}. Not all of these are equally important for linear collider studies. The operators O_{qW} and $O^3_{\Phi q}$ are severely constrained by the LEP1 observables R^b and $A^b_{\rm FB}$. The remaining operators are so far not directly constrained by any experimental data. Bounds from partial wave unitarity arguments can be found in [29]. The operator O_{t3} has the same structure as a dimension 4 right-handed current and is strongly restricted for reasons given in [27]. The operators O_{Dt} and O_{Db} include the derivatives of the t and b fields. If one applies the equations of motion to them [30], they can be expressed within another class of effective operators.

So only the $O_{bW\Phi}$ and $O_{tW\Phi}$ operators remain:

$$O_{tW\Phi} = [(\bar{q}_{\rm L}\sigma^{\mu\nu}\tau^I t_{\rm R})\Phi + \Phi^+(\bar{t}_{\rm R}\sigma^{\mu\nu}\tau^I q_{\rm L})]W^I_{\mu\nu}, \quad (4)$$

$$O_{bW\Phi} = [(\bar{q}_{\rm L}\sigma^{\mu\nu}\tau^I b_{\rm R})\Phi + \Phi^+(\bar{b}_{\rm R}\sigma^{\mu\nu}\tau^I q_{\rm L})]W^I_{\mu\nu}. \quad (5)$$

Here $q_{\rm L}$ is the left-handed third-family doublet, Φ is the Higgs boson doublet, $\tau^I = \sigma^I/2$, $W_\mu = \tau^I W^I_\mu$. In the unitary gauge the following effective $Zb\bar{b}$, $\gamma b\bar{b}$, $Wt\bar{b}$, $Zt\bar{t}$ and $\gamma t\bar{t}$ Lagrangian terms appear after symmetry breaking and the rotation to physical fields $(W^3_\mu, B_\mu) \to (Z_\mu, A_\mu)$

$$\mathcal{L}_{Wt\bar{b}} = \frac{C_{tW\Phi}}{\Lambda^2}\frac{v}{2}W^+_{\mu\nu}(\bar{t}\sigma^{\mu\nu}P_{\rm L}b) + \frac{C_{bW\Phi}}{\Lambda^2}\frac{v}{2}W^+_{\mu\nu}(\bar{t}\sigma^{\mu\nu}P_{\rm R}b), \quad (6)$$

$$\mathcal{L}_{Zb\bar{b}} = \frac{C_{bW\Phi}}{\Lambda^2}\frac{c_{\rm W}}{2}\frac{v}{\sqrt{2}}Z_{\mu\nu}\bar{b}\sigma^{\mu\nu}b, \quad (7)$$

$$\mathcal{L}_{\gamma b\bar{b}} = -\frac{C_{bW\Phi}}{\Lambda^2}\frac{s_{\rm W}}{2}\frac{v}{\sqrt{2}}A_{\mu\nu}\bar{b}\sigma^{\mu\nu}b, \quad (8)$$

$$\mathcal{L}_{Zt\bar{t}} = -\frac{C_{tW\Phi}}{\Lambda^2}\frac{c_{\rm W}}{2}\frac{v}{\sqrt{2}}Z_{\mu\nu}\bar{t}\sigma^{\mu\nu}t, \quad (9)$$

$$\mathcal{L}_{\gamma t\bar{t}} = \frac{C_{tW\Phi}}{\Lambda^2}\frac{s_{\rm W}}{2}\frac{v}{\sqrt{2}}A_{\mu\nu}\bar{t}\sigma^{\mu\nu}t, \quad (10)$$

where Λ is the scale of new physics, $v(g^2+g'^2)^{1/2} = 2m_Z$, $s^2_{\rm W} = 1 - m^2_W/m^2_Z$ and the C's denote the couplings. The corresponding Lagrangian is only $U(1)$ invariant. So, if we start from the $SU(2) \times U(1)$ invariant operators (4) and (5), the introduction of the anomalous couplings $C_{bW\Phi}$ and $C_{tW\Phi}$ in a gauge invariant manner inevitably gives also anomalous contributions to the $Vb\bar{b}$ and $Vt\bar{t}$ ($V = \gamma, Z$) vertices (6)–(10) involving the same couplings. After the redefinition of the anomalous couplings $f_{2\rm L}$ and $f_{2\rm R}$ in (3)

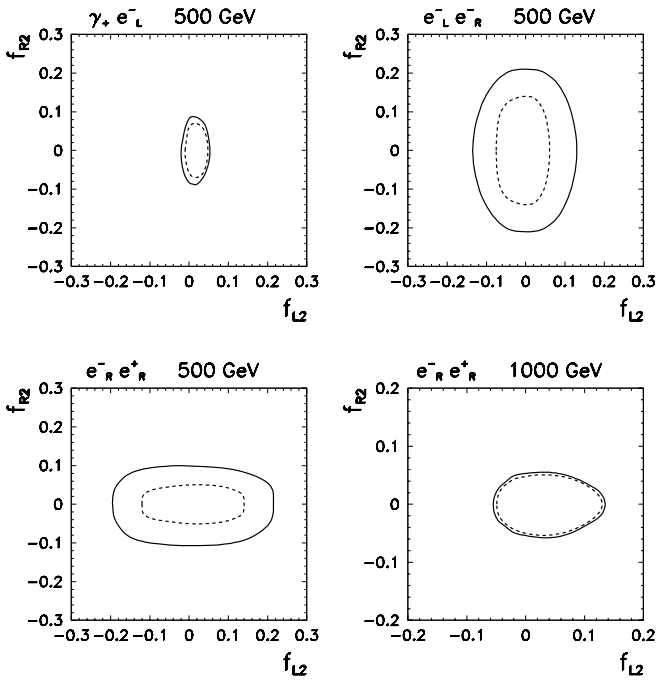

Fig. 13. 2σ bounds on the anomalous couplings $f_{2\rm L}$ and $f_{2\rm R}$ from the reactions $\gamma_+ e^-_{\rm L} \to \nu_e\bar{t}b$, $e^-_{\rm L}e^-_{\rm R} \to e^-\nu_e\bar{t}b$ and $e^-_{\rm R}e^+_{\rm R} \to e^-\bar{\nu}_e t\bar{b}$ at $s^{1/2} = 0.5\,\text{TeV}$ and $1.0\,\text{TeV}$, for integrated luminosities of $100\,\text{fb}^{-1}$ (solid lines) and $500\,\text{fb}^{-1}$ (dashed lines)

$$f_{2\rm L} = \frac{C_{tW\Phi}}{\Lambda^2}\frac{v\sqrt{2}m_W}{g}, \quad f_{2\rm R} = \frac{C_{bW\Phi}}{\Lambda^2}\frac{v\sqrt{2}m_W}{g}, \quad (11)$$

we obtain exactly the effective Wtb term (6).

Usually, in analyses of anomalous couplings the lowest order s-channel diagrams with only one anomalous vertex are calculated in the *production* × *decay* approximation. However, in our case of three and four fermion final states, gauge invariant subsets of diagrams with all five effective vertices (6)–(10) exist, and $SU(2)$ symmetry conserving calculations should account for all vertices (6)–(10) at the same time. Such calculations are beyond our present techniques. Existing experience of SM calculations in approaches where $SU(2)$ symmetry is violated result in an increase of cross sections by a factor of 2 to 3. This discrepancy is not so dramatic as in the case of broken $U(1)$, with deviations of several orders of magnitude.

So a consistent and rigorous investigation of top quark physics induced by $SU(2) \times U(1)$ invariant local operators (4) and (5) is, generally speaking, nontrivial and requires careful additional studies. It is interesting to analyze the sensitivity of the helicity suppressed SM processes (like $\gamma e^-_{\rm R} \to \nu_e\bar{t}b$ or $e^+_{\rm L}e^-_{\rm L} \to e^-\bar{\nu}_e t\bar{b}$) to anomalous effective operators which could destroy such a m^2_e/s suppression and might lead to observable cross sections.

4 Conclusions

Top quark physics will be one of the central issues of the physics program for a next linear collider. In partic-

ular, nonstandard phenomena are expected to be most pronounced in the top quark sector [31]. As discussed in this paper and elsewhere, single top quark production processes imply distinct advantages in measurements of the V_{tb} matrix element and the structure of the Wtb vertex.

Taking into account the variety of possible collision modes for the LC (e^+e^-, e^-e^-, γe^-, $\gamma\gamma$), combined with all possibilities of different beam polarizations, we performed single top cross section evaluations for the complete sets of the SM tree-level diagrams. From comparisons of the possible production rates we conclude that the extremely favored single top production process is $\gamma e \to \nu_e \bar{t} b$, especially in the case of polarized collisions. Precise cross section measurements are accessible due to large counting rates and the absence of $t\bar{t}$ pair production. The best option in γe collisions is found when circular polarized (+) photons collide with left-handed electrons, at the largest possible energy. In this case, $\sigma(\gamma_+ e_{\rm L} \to \nu_e \bar{t} b)$ is close to 100 fb at 0.5 TeV and grows to about 170 fb at 1 TeV c.m.s. energy. Thanks to the proportionality of $\sigma(\gamma e \to \nu_e \bar{t} b)$ to the CKM matrix element V_{tb}, unrivaled precision can be achieved for the latter.

The process $e^-e^- \to e^-\nu_e \bar{t} b$ is also appropriate for precise single top cross section measurements. Here the clean environment, the relatively simple switchover mechanism from e^+e^- to e^-e^- collisions, the absence of $t\bar{t}$ pair production and the large electron polarization degree combined with cross sections of ≥ 2 fb make this process promising.

Reactions like $e^+e^- \to e^-\bar{\nu}_e t\bar{b}$ and $\gamma\gamma \to e^-\bar{\nu}_e t\bar{b}$ are less favored for single top quark physics. The separation of the $t\bar{t}$ production, typically about two orders of magnitude larger than single top rates, dilutes the precision of single top quark cross section determination. Even if both e^+ and e^- are right-polarized, so that no $t\bar{t}$ production is possible, imperfect polarizations degrade significantly a precise $e^+_{\rm R}e^-_{\rm R} \to e^-\bar{\nu}_e t\bar{b}$ event rate measurement.

As an illustrative example of the objectives of single top quark production processes we analyzed their sensitivity to anomalous Wtb couplings $f_{2\rm L}$, $f_{2\rm R}$ of the effective dimension 6 Lagrangian. A large single top cross section does not necessarily provide better sensitivity to anomalous couplings. We selected from all possibilities the following reactions: $\gamma_+ e^-_{\rm L} \to \nu_e \bar{t} b$, $e^+_{\rm R}e^-_{\rm R} \to e^-\bar{\nu}_e t\bar{b}$ and $e^-_{\rm L}e^-_{\rm R} \to e^-\nu_e \bar{t} b$, since they are relatively simple and free of $t\bar{t}$ background. At $s^{1/2} = 0.5$ TeV and assuming $100\,{\rm fb}^{-1}$ or $500\,{\rm fb}^{-1}$ integrated luminosity, best bounds for $f_{2\rm L}$ ($-0.02 \leq f_{2\rm L} \leq 0.06$) were found for the reaction $\gamma_+ e^-_{\rm L} \to \nu_e \bar{t} b$. The coupling $f_{2\rm R}$ is expected to be almost equally well bounded ($-0.1 \leq f_{2\rm R} \leq 0.1$) by $\gamma_+ e^-_{\rm L}$ and $e^+_{\rm R}e^-_{\rm R}$ collisions, with the potential for improvements to $-0.05 \leq f_{2\rm R} \leq 0.05$ in the fully polarized $e^+_{\rm R}e^-_{\rm R} \to e^-\bar{\nu}_e t\bar{b}$ channel for $500\,{\rm fb}^{-1}$ integrated luminosity. These bounds are comparable or somewhat improved to those from $t\bar{t}$ studies, where sophisticated combinations of asymmetries [21] are needed to probe the anomalous Wtb vertex.

We are aware that our results rely on tree-level calculations and it would be desirable to include next-to-leading order and initial state radiation corrections, beamstrahlung and to account for a realistic backscattered photon spectrum. We however do not expect that our conclusions will be qualitatively affected by more elaborate calculations.

Acknowledgements. The work of E.B., M.D. and A.P. was partially supported by RFBR-DFG grant 00-02-04011, RFBR grant 01-02-16710, scientific program "Universities of Russia" grant 990588, CERN-INTAS grant 99-0377 and INTAS grant 00-00679. E.B. and M.D. thank very much DESY-Zeuthen for hospitality.

References

1. Top quark physics, in: e^+e^- collisions at 500 GeV: the physics potential, edited by P.M. Zerwas, DESY 92-123A, p. 255, DESY 93-123C, p. 245, DESY 96-123D, p. 1, DESY 97-123E, p. 3
2. S. Ambrosanio, B. Mele, Z. Phys. C **63**, 63 (1994) (hep-ph/9311263)
3. N.V. Dokholian, G.V. Jikia, Phys. Lett. B **336**, 251 (1994)
4. M. Katuya, J. Morishita, T. Munehisa, Y. Shimizu, Progr. Theor. Phys. **75**, 92 (1986)
5. K. Hagiwara, M. Tanaka, T. Stelzer, Phys. Lett. B **325**, 521 (1994); E. Boos, M. Sachwitz, H.J. Schreiber, S. Shichanin, A. Pukhov, V. Ilyin, T. Ishikawa, T. Kaneko, S. Kawabata, Y. Kurihara, Y. Shimizu, H. Tanaka, Phys. Lett. B **326**, 190 (1994)
6. E. Boos, Y. Kurihara, M. Sachwitz, H.J. Schreiber, S. Shichanin, Y. Shimizu, Z. Phys C **70**, 255 (1996)
7. A. Bienarchik, K. Cieckiewicz, K. Kolodziej, hep-ph/0102253
8. E. Boos, A. Pukhov, M. Sachwitz, H.J. Schreiber, Phys. Lett. B **404**, 119 (1997) (hep-ph/9610424)
9. M.C. Smith, S. Willenbrock, Phys. Rev. D **54**, 6696 (1996) (hep-ph/9604223); A.P. Heinson, A.S. Belyaev, E.E. Boos, Phys. Rev. D **56**, 3114 (1997) (hep-ph/9612424); T. Stelzer, Z. Sullivan, S. Willenbrock, Phys. Rev. D **56**, 5919 (1997) (hep-ph/9705398); T. Tait, C.-P. Yuan, MSUHEP-71015, hep-ph/9710372; A.S. Belyaev, E.E. Boos, L.V. Dudko, Phys. Rev. D **59**, 075001 (1999) (hep-ph/9806332); E. Boos, L. Dudko, T. Ohl, Eur. Phys. J. C **11**, 473 (1999) (hep-ph/9903215)
10. E. Boos, M. Dubinin, V. Ilyin, A. Pukhov, V. Savrin, INP MSU 94-36/358, 1994 (hep-ph/9503280); P. Baikov et al., in: Proceedings of X Workshop on High Energy Physics and Quantum Field Theory, edited by B. Levtchenko, V. Savrin, Moscow, 1996, p. 101 (hep-ph/9701412); A. Pukhov et al., hep-ph/9908288; see also http://theory.npi.msu.su/comphep
11. E. Accomando, A. Ballestrero, M. Pizzio, Nucl. Phys. B **512**, 19 (1998) (hep-ph/9706201); F. Yuasa, Y. Kurihara, S. Kawabata, Phys. Lett. B **414**, 178 (1997) (hep-ph/9706225)
12. A. Ballestrero, E. Maina, S. Moretti, Phys. Lett. B **333**, 434 (1994) (hep-ph/9404338); A. Ballestrero, E. Maina, S. Moretti, Phys. Lett. B **333**, 460 (1994) (hep-ph/9409291)
13. D. Bardin, R. Kleiss et al., in: Physics at LEP2, edited by G. Altarelli, T. Sjoestrand, F. Zwirner, CERN report 96-01, 1996, vol. II (hep-ph/9709270)

14. E. Boos, T. Ohl, Phys. Rev. Lett. **83**, 480 (1999) (hep-ph/9903357)
15. A. Belyaev, E. Boos, Phys. Rev. D **63**, 034012 (2001) (hep-ph/0003260)
16. M. Grunewald, G. Passarino et al., in: Reports of the working groups on precision calculations for LEP2 Physics, edited by R. Pittau, CERN Yellow Report 2000-0009, 2000 (hep-ph/0005309); G. Passarino, in: Proceedings of 30th International Conference on High Energy Physics, Osaka, Japan, 2000 (hep-ph/0009249)
17. M. Beneke et al., Top quark physics, in: Proceedings of the Workshop on Standard Model Physics at the LHC, edited by G. Altarelli, M. Mangano, CERN 2000-04 (hep-ph/0003033)
18. G.V. Jikia, Nucl. Phys. B **374**, 83 (1992); J.-J. Cao, J.-X. Wang, J. Yang, B.L. Young, X. Zhang, Phys. Rev. D **58**, 094004 (1998) (hep-ph/9804343)
19. P. Comas, R. Miquel, M. Martinez, S. Orteu, CERN-PPE/96-40
20. T.M. Tait, Phys. Rev. D **61**, 034001 (2000) (hep-ph/9909352)
21. E. Boos, M. Dubinin, M. Sachwitz, H.J. Schreiber, Eur. Phys. J. C **16**, 269 (2000) (hep-ph/0001048)
22. C. Schmidt, Phys. Rev. D **54**, 3250 (1996) (hep-ph/9504434); R. Frey, in: Proceedings of the Workshop on Physics and Experiments with Linear Colliders, Morioka-Appi, Japan, 1995 (hep-ph/9606201); B. Grzadkowski, Z. Hioki, Phys. Rev. D **61**, 014013 (2000) (hep-ph/9805318); B. Grzadkowski, Z. Hioki, Nucl. Phys. B **585**, 3 (2000) (hep-ph/0004223)
23. G. Kane, G. Ladinsky, C.-P. Yuan, Phys. Rev. D **45**, 124 (1992)
24. Y. Kurihara, D. Perret-Gallix, Y. Shimizu, Phys. Lett. B **349**, 367 (1995) (hep-ph/9412215)
25. E. Boos, M. Dubinin, in: Proceedings of the XIV International Workshop on High Energy Physics and Quantum Field Theory (QFTHEP'1999), edited by B. Levtchenko, V. Savrin, Moscow, 2000 (hep-ph/9909214)
26. J. Hoogland, Geert Jan van Oldenborgh, Phys. Lett. B **402**, 379 (1997) (hep-ph/9702441)
27. T.M.P. Tait, C.-P. Yuan, Phys. Rev. D **63**, 014018 (2001) (hep-ph/0007298)
28. K. Whisnant, J.M. Yang, B.-L. Young, X. Zhang, Phys. Rev. D **56**, 467 (1997) (hep-ph/9702305)
29. G. Gounaris, D. Papadamou, F. Renard, Z. Phys. C **76**, 333 (1997) (hep-ph/9609437)
30. W. Buchmuller, D. Wyler, Nucl. Phys. B **268**, 621 (1986)
31. R.D. Peccei, X. Zhang, Nucl. Phys. B **337**, 269 (1990); R.D. Peccei, S. Peris, X. Zhang, Nucl. Phys. B **349**, 305 (1991)